Scaling Relations on Basal Plane Vacancies of Transition Metal Dichalcogenides for CO2 Reduction

Ji, Yongfei; Nørskov, Jens K.; Chan, Karen

Published in:
Journal of Physical Chemistry C

Link to article, DOI:
10.1021/acs.jpcc.8b11628

Publication date:
2019

Document Version
Peer reviewed version

Scaling relations on Basal Plane Vacancies of Transition Metal Dichalcogenides for CO_2 Reduction

Yongfei Ji[†‡%], *Jens K. Nørskov*[#], *Karen Chan*[#*]

[†]*SUNCAT Center for Interface Science and Catalysis, SLAC National Accelerator Laboratory, 2575 Sand Hill Road, Menlo Park, California 94025, USA.*

[‡]*SUNCAT Center for Interface Science and Catalysis, Department of Chemical Engineering, Stanford University, Stanford, California 94305, USA.*

[%] *Department of Chemistry and Chemical Engineering, Guangzhou University, 230 Wai Huan Xi Road,Guangzhou Higher Education Mega Center, Guangzhou, 510006, P. R. China*

[#]*Catalysis Theory Center, Department of Physics, Technical University of Denmark, Lyngby, Denmark 2820*

ABSTRACT. Transition metal dichalcogenides (TMDs) have shown promising electrocatalytic performance for CO_2 reduction (CO_2R) recently. However, the development of efficient and selective catalysts remains a major challenge. While recent studies have suggested the importance of activation energies as activity descriptors for CO_2R beyond CO, the scaling of intermediate binding energies present a first step in computational catalyst screening. Here, we investigate the

basal vacancy on 2H and 1T/1T' phase group V, VI and X TMDs for CO_2 reduction. We find that the change of oxophicility and carbophilicity on each group of TMDs follow different trends, which leads to different scaling relations amongst key intermediates. Our thermochemical analysis also suggests Group V and VI TMDs to be either selective for hydrogen evolution reaction (HER) or prone to OH poisoning. However, the initial analysis suggests group X TMDs to be possible candidates for active and selective CO_2 reduction without suffering from OH poisoning, which motivates further theoretical kinetic studies. We furthermore find that their reaction energetics can be tuned by the density of the basal vacancies.

Introduction

Electrochemical reduction of CO_2 to value-added organic molecules has attracted intensive attention as a potential way to mitigate the energy and environmental crisis. Recently, transition metal dichalcogenides (TMDs) have been suggested to be electrochemically active for CO_2 reduction (CO_2RR)[1–4]. Asadi *et al.* reported CO_2 to CO on group VI TM sulfides and selenides with a selectivity of 24% at a low overpotential of 54 millivolts[1]; Liu *et al.* found that $MoTe_2$ can electrochemically reduce CO_2 to CH_4 with a selectivity of 84% at -1.0 V_{RHE} at relatively high current density[3]; Xu *et al.* found that the selectivity can be tuned by alloying Se with MoS_2 to form MoSSe, which can boost the reduction of CO_2 to syngas[4]. The active sites of TMDs have been suggested to be the edge sites[2,5] which can be easily doped with transition metals[1,4]. Abbasi *et al.* found that Nb doped MoS_2 can promote CO_2 reduction to CO whereas the Ta doping shows negative effects[6]. To suppress hydrogen evolution (HER), all these measurements were conducted in 1-ethyl- 3-methylimidazolium tetrafluoroborate (EMIM-BF_4), which has been suggested to bind CO_2 and lower the overpotential[7] for CO_2RR, to exert a field-induced stabilization of the

intermediates[8] or to provide a source of protons for transfer[9]. On the other hand, $EMIM^+$ cations have been shown to degrade under the reaction condition which can affect the measured CO_2RR product distribution and therefore necessitates the use of isotope labelling.[10]

To deconvolute the effect of the ionic liquid from the intrinsic activity of these catalysts, a combined experimental and theoretical study in aqueous condition[11] on nine TM phosphides and five TMDs was performed. In all the ionic compounds considered, the predominant product was found to be H_2. The selectivity towards H_2 was investigated computationally and found to either arise from low thermodynamic limiting potentials for HER relative to CO_2RR or, in the case of the TMDs, to arise from poor scaling of the critical H-CO transition state from proton-electron transfer to CO.

The activity of the basal planes of TMDs has, to date, been unexplored for its potential for CO_2RR. Although the density of sites on the basal plane are high, there are generally inert. However, Tsai *et al.* showed that the basal plane of TMDs can be activated for HER by creating chalcogen vacancies[12,13], and the binding energy of the intermediates can be tuned by the density of the chalcogen vacancy and in-plane strain which change the number of gap states and density of states near fermi level. This presents a potential method for tuning the activity and selectivity of TMDs for CO_2RR. On the other hand, because the vacancy of the TMDs expose three low-coordinated TM atoms, the interaction with the adsorbates may differ from those at the edge sites and result in new scaling relations amongst binding energies. Currently, only the basal plane vacancies of group VI TMDs in the 2H phase (figure 1) have been investigated for HER.

In this work, we perform an initial thermochemical screening of the 2H and 1T/1T' (figure 1) sulfides and selenides for CO_2RR. We consider group V and VI sulfides in the 2H phase, and

group V, VI, and X in the 1T phase, since group X TMDs only exist in 1T phase. As in our previous works[14,15], we will focus on the scaling relations between the formation energies of the intermediates (E(COOH*), E(CHO*) and E(CO*)) in the first three key steps for CO_2 reduction (reaction (1-3)).

$$CO_2 + H^+ + e^- + * \rightarrow COOH^* \quad (1)$$

$$COOH^* + H^+ + e^- \rightarrow CO^* + H_2O \quad (2)$$

$$CO^* + H^+ + e^- \rightarrow CHO^* \quad (3)$$

We find that the scaling relations on TMDs are different from those on pure TMs and the oxygen and carbon affinity play important role in forming different scaling relation among different group TMDs. We also evaluate the thermochemistry for the competitive hydrogen evolution reaction (HER) and the propensity for OH poisoning (See Supporting Information). Overall, the thermochemical analysis suggests group X TMDs to be potential candidates for efficient CO_2 reduction with high selectivity and resistance to OH poisoning, which motivates further detailed theoretical studies of their corresponding kinetic barriers. Furthermore, we found that the electrocatalytic performance can be tuned by increasing the density of basal vacancies.

Theoretical Methods

All calculations were carried out using density functional theory implemented in Quantum Espresso with periodic boundary conditions[16], using plane-wave basis sets[17] and ultrasoft pseudopotentials[18], interfaced with the Atomic Simulation Environment[19]. The Bayesian error estimation exchange-correlation functional with van der Waals interactions (BEEF-vdW)[20], which is optimized for chemisorption energies and van der Waals interactions, was used with a plane-

wave cutoff of 500eV and a density cutoff of 5000 eV. A rectangular (4x4) supercell with a vacuum of 11Å was used for calculation. The Brillouin zone was sampled with a (2x2x1) Monkhorst-pack grid K-points. All atoms were relaxed until the maximum force on the atoms is smaller than 0.05 eV/ Å. A dipole correction in the z direction was used[21]. The computational hydrogen electrode[22] was used to calculate the free energy of formation of the intermediates as in previous works[14,15]. Solvent stabilizations of 0.25 eV, 0.1 eV, 0.1 eV and 0.25 eV were applied to the binding energies of COOH*, CO*, CHO* and OH* respectively[23].

Fig. 1 shows the structure of the TMDs in both the 2H and 1T phases. In both cases, the metal atoms are six-fold coordinated to the chalcogens. The difference between the two phases is that the chalcogens are coordinated in a trigonal prismatic arrangement in the 2H phase and in an octahedral arrangement in the 1T phase. In our investigations of the effect of defect densities on group X TMD in the 1T phase (cf. Fig. 5), vacancies were removed following the order of the number shown in the top schematic of the 1T phase.

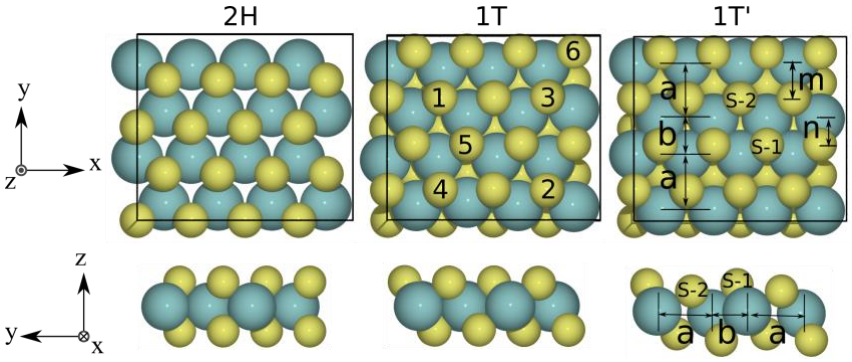

Figure 1. Structures of single layer transition metal dichalchogenides in 2H, 1T and 1T' phase. Green and yellow spheres stand for metal and chalcogen atoms. In our investigations of the effect of defect densities on group X TMD (cf. Fig. 5), vacancies were removed following the order of the number shown in the middle figure.

The group VI TMDs in the 1T phase undergoes a (1x2) reconstruction spontaneously to the 1T' phase. In this phase, the vertical distances between the rows of the transition metals alternates between "a" and "b" as illustrated in Fig .1[24,25]. This reconstruction creates two inequivalent chalcogen vacancies marked S-1 and S-2 in Figure 1. Table S1 summarizes the formation energies of the S-1 and S-2 vacancies on the group VI TMDs in the 1T'-phase. Removing S-2 is always more facile, as it has larger bond distances to the coordinating transition metal atoms than S-1, as illustrated in Fig. 1 (distance *m* > distance *n*). Thus, we only consider the adsorption of the intermediates at the S-2 vacancy. We have considered various binding configurations of the intermediates, and explore the scaling relations determined from the most stable ones.

Results and Discussion

Scaling Relations

Figure 2(a) shows the scaling relations and the most stable structures of the intermediates COOH*, CO*, and CHO* adsorbed on the vacancy of all the TMDs (OH* and H* are shown in Figure S1). Because the adsorbates bind with similar configurations within the same group of TMDs, the structures for each group are exemplified by one compound: group V by VS_2, group VI by MoS_2 and group X by PtS_2. *COOH adsorbs on the 2H-VI and 1T-X TMDs in a top-bridge (C atop, O on bridge) geometry, but on other TMDs in a top-top (C atop, O atop) geometry; CO* adsorbs on 2H-VI TMDs at the hollow site, on 1T-X TMDs at the bridge site and on other TMDs at the top site; CHO* adsorbs on the 2H-VI and TMDs with a bridge-top (C on bridge, O atop) geometry, but on the 1T'-VI TMDs in the top-bridge (C atop, O on bridge) configuration, and on other TMDs with a top-top geometry. E(COOH*) and E(CHO*) are known to scale well with E(CO*) on TM

surfaces. In contrast, Figures 2(b) and (c) show that TMDs show significant differences in scaling amongst the different groups and phases. These differences do not arise solely from differences in the adsorption structures of the intermediates. For example, the 2H-V, 1T-V and 1T-VI' TMDs show similar binding configurations for COOH* and CO*, but very different scaling lines.

Similarly, 2H-V and 1T-V TMDs show similar binding configurations for CHO* and CO* but again different scaling lines.

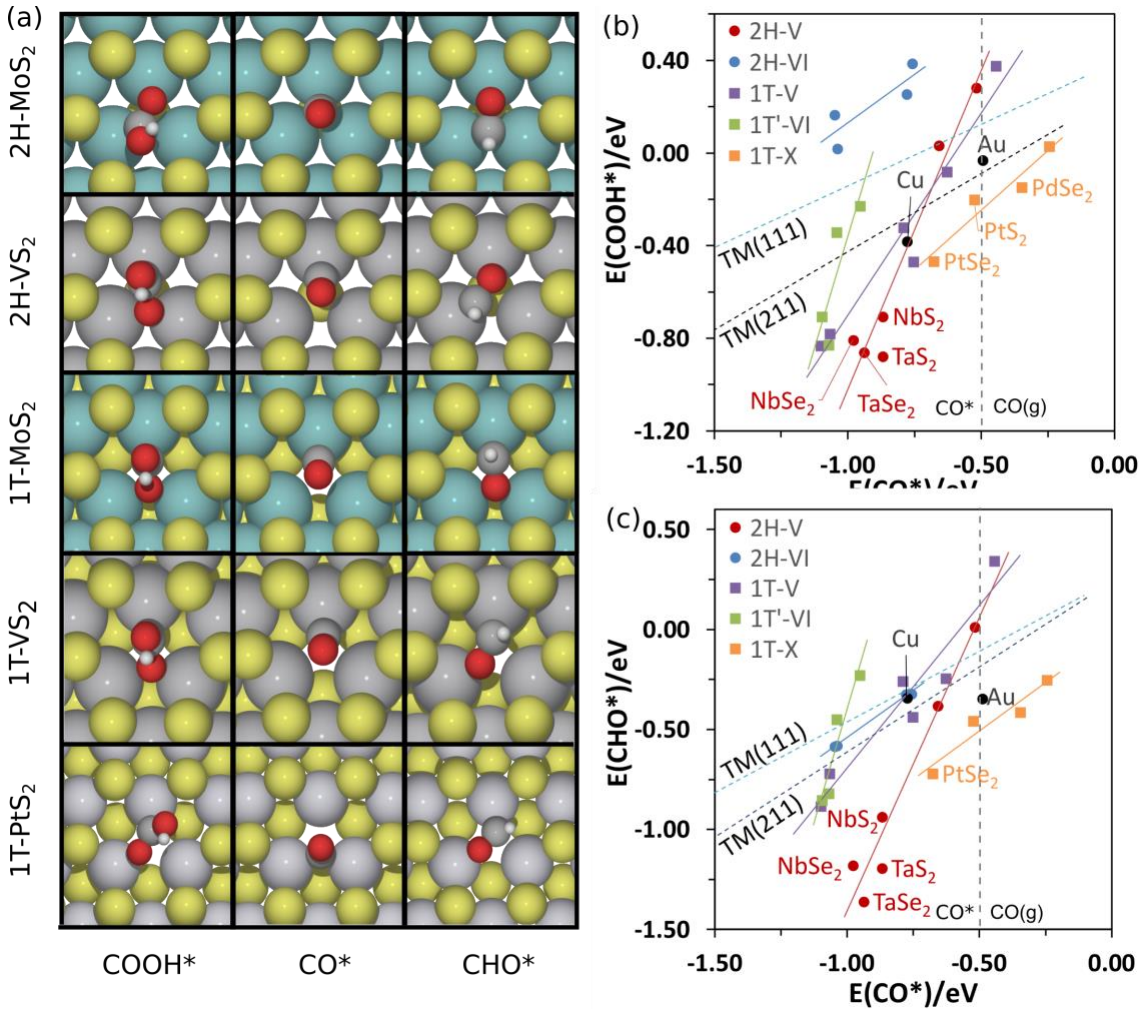

Figure 2, (a) Adsorption structures of the intermediates; scaling relation of E(COOH*) and E(CHO*) with E(CO*). For clarity, only part of the data points are labeled in (b) and (c), figures with full labels can be found in Figure S2. The vertical dashed lines indicate the E (CO*) at which an isolated *CO is in equilibrium with 0.01 bar gaseous CO. The catalysts to the right of the line tend to bind CO weakly and are expected to be selective for CO production. The catalysts to the left may able to further reduce CO*.

The differences in the oxophilicity of the different groups and phases, on the other hand, can be shown to contribute to the differences amongst the scaling lines. Since the COOH* are bonded

to the TM atoms via the C and O atoms, E(COOH*) scales with the binding energies of C- and O-bound species, for example CO* and OH*:

$$E(COOH^*) = \alpha E(CO^*) + \beta E(OH^*) + \gamma \quad (4)$$

For E(COOH*) and E(CHO*) to scale with E(CO*), E(OH*) must scale with E(CO*) as well:

$$E(CO^*) = \kappa E(OH^*) + \lambda \quad (5)$$

$$E(COOH^*) = (\alpha + \kappa\beta)E(CO^*) + \gamma' \quad (6)$$

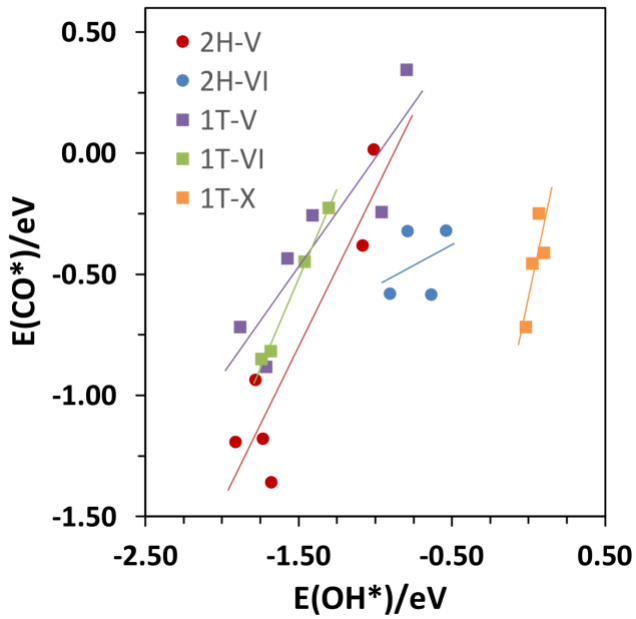

Figure 3. Scaling relation between E(CO*) with E(OH*). A figure with full labeling of all points can be found in Figure S3

As shown in Figure 3, different E(CO*)-E(OH*) scaling lines form for each group TMDs. From linear fits (R_2 values in Table S2), E(CO*) scale well with E(OH*) except on the 2H-VI TMDs, which is probably why they do not scale well with E(COOH*) on 2H-VI TMDs (Figure 2). Generally, E(OH*) do not scale with E(CO*) on TM surfaces[26,27], but they may scale within

the same class of material. For example, a good linear correlation has been found between E(O*) and E(C*) on the Pd alloys[28]. Therefore, it is since the oxophilicity and carbophilicity of the TMDs vary with group and phase, the various groups and phases also show different E(COOH*)-E(CO*) scaling relations. Along the same vein, scaling relations on the early transition metal carbides have also been found to depart from the transition metal surfaces because they show different oxophilicity/carbophicility from their parent transition metals[29]. The departure was rationalized with the adsorbate-surface valence configuration and the energy of the metal *sp*-states, rather than metal *d*-states that govern the scaling relation of pure transition metals.

From the scaling relations in Figure 2(b) and (c), several materials can be potential candidates for efficient CO_2 reduction to CO and further CO reduction. From Figure 2(b), PtS_2 and $PdSe_2$ may be more active than Au(211) for CO_2 reduction to CO because they have lower E(COOH*) than Au(211) but do not bind CO. According to Figure 2(c), $PtSe_2$, and 2H phase Nb and Ta dichalcogenides may have some potential to reduce CO further, since they bind CO stronger or similarly to Cu but with significantly reduced CHO* energies. The transition state, however, must be evaluated since it does not necessarily scale with the binding energy of CHO*[11].

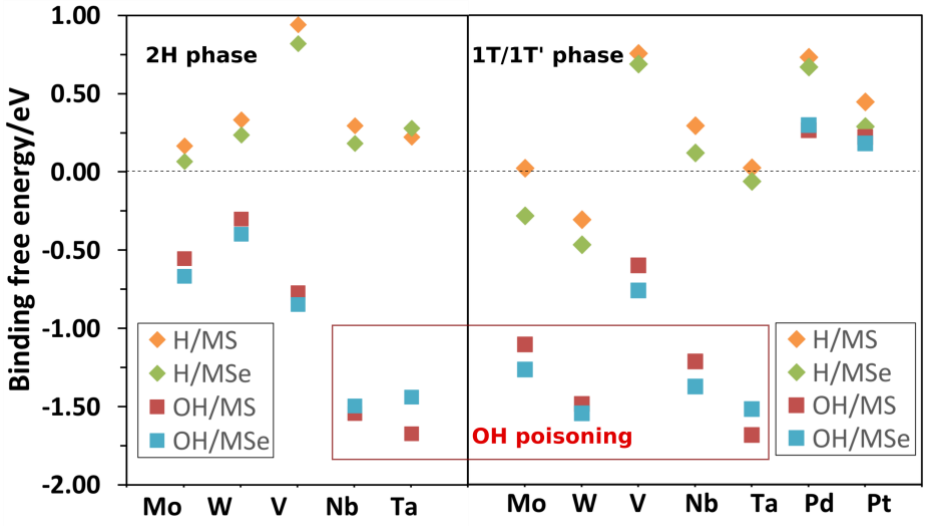

Figure 4, Binding free energies at the basal vacancy of the 2H and 1T/1T' phase TMDs

To consider the competition with HER and the propensity for OH poisoning, we show the binding free energies of H* and OH* at 0.0 V_{RHE} in Figure 4 (structures in Figure 2). 2H-$MoSe_2$, 1T'-MoS_2, 1T-$NbSe_2$, 1T-TaS_2 and 1T-$TaSe_2$ are suggested to be efficient catalysts for HER since the $\Delta G(H^*)$ on them is close to thermoneutral[30]. On the other hand, $\Delta G_o(OH^*)$ on Nb, Ta dichalcogenides (1T and 2H), Mo and W 1T'-dichalcogenides are lower than -1.0 eV, which suggests that they may suffer from OH poisoning down to reducing potentials of -1V vs. RHE (See Supporting Information). Therefore, among all the candidates, only the group X TMDs, and in particular the PtS_2 and $PtSe_2$, are suggested by the thermochemical analysis to have potential to be active and selective for CO_2R and be resistant to OH poisoning.

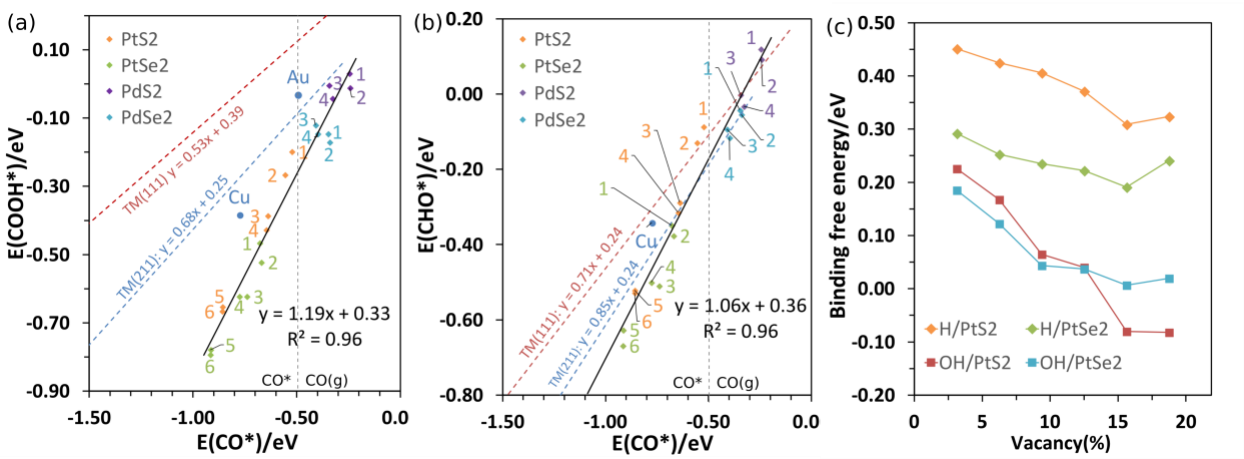

Figure 5(a) and (b): Scaling relations of group X TMDs with various densities of basal plane vacancies. The labels show the number of vacancies removed in 4x4 cells. (c), The change in the binding free energies of H and OH with the density of vacancies.

Finally, we investigate the effect of changing the density of basal vacancy on the scaling relations on group X TMDs. As shown in Figure 5, the binding of the intermediates change slightly with the density of vacancy on PdS_2 and $PdSe_2$, but change significantly on PtS_2 and $PtSe_2$. Therefore, $PdSe_2$ remains a candidate for CO_2R to CO, whereas PtS_2 at a high vacancy density and $PtSe_2$ can bind CO and may be capable of reducing it further. Because CO* is formed via COOH*,

the thermodynamic limiting potential to form CO* will decrease with increasing densities of vacancies; in addition, because the slope of the E(CHO*)-E(CO*) scaling is larger than 1 (Figure 5(b)), the thermodynamic limiting potential to form CHO* also decreases with increasing density[26]. Therefore, in the moderate CO binding regime, the activity of these materials is suggested to increase with the density of the vacancy. Since the slopes of the scaling relations are larger than those on TM(211) surfaces, and scaling lines lie below the TM(211) scaling lines, the present analysis suggests the vacancy on Pt dichalcogenides to be more active than the TM(211) surface, though the transition state should also be evaluated[11]. At the same time, the formation energies of H* and OH* are less sensitive to the density of the vacancy (Figure 5(c)), so the material should remain resistant to HER and OH poisoning. However, if the density of the vacancy becomes too high, the material would strongly bind CO and be poisoned by it, as in the case of strong binding metals for CO_2RR.

Conclusions

In summary, we have investigated the basal vacancies group V, VI and X transition metal dichalcogenides in 2H and 1T/1T' phases for electrochemical reduction of CO_2 by exploring the scaling relations of the key intermediates. Because of the difference in the oxygen affinity, the scaling relations deviate from transition metal ones and also show variations amongst TMDs of different groups and phases. Most of the TMDs were found to be either active for HER or prone to OH poisoning. Only group X TMDs are suggested to be active and selective candidates for CO_2 reduction without suffering from OH poisoning. Furthermore, our calculations suggest that the performance can be improved and the selectivity and be tuned by increasing the density of basal

vacancy. This work motivates further theoretical study including transition states and associated kinetics of the relevant intermediates and experimental testing of group X TMDs.

Corresponding Author

*kchan@fysik.dtu.dk

Present Addresses

†If an author's address is different than the one given in the affiliation line, this information may be included here.

Funding Sources

Supporting Information

Definition of OH poisoning effect; formation energy of S vacancies; adsorption structures of OH* and H*; fully labeled figures and binding energies of all intermediates summarized in tables; parameters of the linearing fitting.

Acknowledgment

This work was supported by the U.S. Department of Energy, Office of Science, Office of Basic Energy Science, via Grant DE-SC0008685 to the SUNCAT Center of Interface Science and Catalysis, as well as the Villum Fonden through a research grant (9455). Y.J. thanks the Knut & Alice Wallenberg Foundation for financial support through the Wallenberg Postdoctoral Scholarship Program.

References

(1) Asadi, M.; Kim, K.; Liu, C.; Addepalli, A. V.; Abbasi, P.; Yasaei, P.; Phillips, P.; Behranginia, A.; Cerrato, J. M.; Haasch, R.; et al. Nanostructured Transition Metal Dichalcogenide Electrocatalysts for CO_2 Reduction in Ionic Liquid. *Science* **2016**, *353*, 467–470.

(2) Asadi, M.; Kumar, B.; Behranginia, A.; Rosen, B. A.; Baskin, A.; Repnin, N.; Pisasale, D.; Phillips, P.; Zhu, W.; Haasch, R.; et al. Robust Carbon Dioxide Reduction on Molybdenum Disulphide Edges. *Nat. Commun.* **2014**, *5, 4470*.

(3) Liu, X.; Yang, H.; He, J.; Liu, H.; Song, L.; Li, L.; Luo, J. Highly Active, Durable Ultrathin $MoTe_2$ Layers for the Electroreduction of CO_2 to CH_4. *Small* **2018**, *14*, 1704049.
(4) Xu, J.; Li, X.; Liu, W.; Sun, Y.; Ju, Z.; Yao, T.; Wang, C.; Ju, H.; Zhu, J.; Wei, S.; et al. Carbon Dioxide Electroreduction into Syngas Boosted by a Partially Delocalized Charge in Molybdenum Sulfide Selenide Alloy Monolayers. *Angew. Chem.* **2017**, *129*, 9249–9253.
(5) Jaramillo, T. F.; Jørgensen, K. P.; Bonde, J.; Nielsen, J. H.; Horch, S.; Chorkendorff, I. Identification of Active Edge Sites for Electrochemical H_2 Evolution from MoS_2 Nanocatalysts. *Science* **2007**, *317*, 100–102.
(6) Abbasi, P.; Asadi, M.; Liu, C.; Sharifi-Asl, S.; Sayahpour, B.; Behranginia, A.; Zapol, P.; Shahbazian-Yassar, R.; Curtiss, L. A.; Salehi-Khojin, A. Tailoring the Edge Structure of Molybdenum Disulfide toward Electrocatalytic Reduction of Carbon Dioxide. *ACS Nano* **2017,** *11***,** 453-460.
(7) Rosen, B. A.; Salehi-Khojin, A.; Thorson, M. R.; Zhu, W.; Whipple, D. T.; Kenis, P. J. A.; Masel, R. I. Ionic Liquid-Mediated Selective Conversion of CO_2 to CO at Low Overpotentials. *Science* **2011**, *334*, 643–644.
(8) Chen, L. D.; Urushihara, M.; Chan, K.; Nørskov, J. K. Electric Field Effects in Electrochemical CO_2 Reduction. *ACS Catal.* **2016**, *6*, 7133–7139.
(9) Wang, Y.; Hatakeyama, M.; Ogata, K.; Wakabayashi, M.; Jin, F.; Nakamura, S. Activation of CO_2 by Ionic Liquid EMIM–BF4 in the Electrochemical System: A Theoretical Study. *Phys. Chem. Chem. Phys.* **2015**, *17*, 23521–23531.
(10) Feaster, J. T.; Jongerius, A. L.; Liu, X.; Urushihara, M.; Nitopi, S. A.; Hahn, C.; Chan, K.; Nørskov, J. K.; Jaramillo, T. F. Understanding the Influence of [EMIM]Cl on the Suppression of the Hydrogen Evolution Reaction on Transition Metal Electrodes. *Langmuir* **2017**, *33*, 9464–9471.
(11) Landers, A. T.; Fields, M.; Torelli, D. A.; Xiao, J.; Hellstern, T. R.; Francis, S. A.; Tsai, C.; Kibsgaard, J.; Lewis, N. S.; Chan, K.; et al. The Predominance of Hydrogen Evolution on Transition Metal Sulfides and Phosphides under CO_2 Reduction Conditions: An Experimental and Theoretical Study. *ACS Energy Lett.* **2018**, *3*, 1450–1457.
(12) Tsai, C.; Li, H.; Park, S.; Park, J.; Han, H. S.; Nørskov, J. K.; Zheng, X.; Abild-Pedersen, F. Electrochemical Generation of Sulfur Vacancies in the Basal Plane of MoS_2 for Hydrogen Evolution. *Nat. Commun.* **2017**, *8*, 15113.
(13) Li, H.; Tsai, C.; Koh, A. L.; Cai, L.; Contryman, A. W.; Fragapane, A. H.; Zhao, J.; Han, H. S.; Manoharan, H. C.; Abild-Pedersen, F.; et al. Activating and Optimizing MoS_2 Basal Planes for Hydrogen Evolution through the Formation of Strained Sulphur Vacancies. *Nat. Mater.* **2016**, *15*, 48–53.
(14) Chan, K.; Tsai, C.; Hansen, H. A.; Norskov, J. K. Molybdenum Sulfides and Selenides as Possible Electrocatalysts for CO_2 Reduction. *Chemcatchem* **2014**, *6*, 1899–1905.
(15) Hong, X.; Chan, K.; Tsai, C.; Nørskov, J. K. How Doped MoS2 Breaks Transition-Metal Scaling Relations for CO_2 Electrochemical Reduction. *ACS Catal.* **2016**, *6*, 4428–4437.
(16) Giannozzi, P.; Baroni, S.; Bonini, N.; Calandra, M.; Car, R.; Cavazzoni, C.; Davide Ceresoli; Chiarotti, G. L.; Cococcioni, M.; Dabo, I.; et al. QUANTUM ESPRESSO: A Modular and Open-Source Software Project for Quantum Simulations of Materials. *J. Phys. Condens. Matter* **2009**, *21*, 395502.
(17) Kresse, G.; Furthmüller, J. Efficiency of Ab-Initio Total Energy Calculations for Metals and Semiconductors Using a Plane-Wave Basis Set. *Comput. Mater. Sci.* **1996**, *6*, 15–50.

(18) Kresse, G.; Hafner, J. Norm-Conserving and Ultrasoft Pseudopotentials for First-Row and Transition Elements. *J. Phys. Condens. Matter* **1994**, *6*, 8245.
(19) Bahn, S. R.; Jacobsen, K. W. An Object-Oriented Scripting Interface to a Legacy Electronic Structure Code. *Comput. Sci. Eng.* **2002**, *4*, 56–66.
(20) Wellendorff, J.; Lundgaard, K. T.; Møgelhøj, A.; Petzold, V.; Landis, D. D.; Nørskov, J. K.; Bligaard, T.; Jacobsen, K. W. Density Functionals for Surface Science: Exchange-Correlation Model Development with Bayesian Error Estimation. *Phys. Rev. B* **2012**, *85*, 235149.
(21) Bengtsson, L. Dipole Correction for Surface Supercell Calculations. *Phys. Rev. B* **1999**, *59*, 12301–12304.
(22) Nørskov, J. K.; Rossmeisl, J.; Logadottir, A.; Lindqvist, L.; Kitchin, J. R.; Bligaard, T.; Jónsson, H. Origin of the Overpotential for Oxygen Reduction at a Fuel-Cell Cathode. *J. Phys. Chem. B* **2004**, *108*, 17886–17892.
(23) Peterson, A. A.; Abild-Pedersen, F.; Studt, F.; Rossmeisl, J.; Nørskov, J. K. How Copper Catalyzes the Electroreduction of Carbon Dioxide into Hydrocarbon Fuels. *Energy Environ. Sci.* **2010**, *3*, 1311–1315.
(24) Duerloo, K.-A. N.; Li, Y.; Reed, E. J. Structural Phase Transitions in Two-Dimensional Mo- and W-Dichalcogenide Monolayers. *Nat. Commun.* **2014**, *5*, 4214.
(25) Tsai, C.; Chan, K.; Nørskov, J. K.; Abild-Pedersen, F. Theoretical Insights into the Hydrogen Evolution Activity of Layered Transition Metal Dichalcogenides. *Surf. Sci.* **2015**, *640*, 133–140.
(26) Peterson, A. A.; Norskov, J. K. Activity Descriptors for CO_2 Electroreduction to Methane on Transition-Metal Catalysts. *J. Phys. Chem. Lett.* **2012**, *3*, 251–258.
(27) Liu, X.; Xiao, J.; Peng, H.; Hong, X.; Chan, K.; Nørskov, J. K. Understanding Trends in Electrochemical Carbon Dioxide Reduction Rates. *Nat. Commun.* **2017**, *8*, ncomms15438.
(28) Xin, H.; Vojvodic, A.; Voss, J.; Nørskov, J. K.; Abild-Pedersen, F. Effects of d -Band Shape on the Surface Reactivity of Transition-Metal Alloys. *Phys. Rev. B* **2014**, *89*, 115114.
(29) Michalsky, R.; Zhang, Y.-J.; Medford, A. J.; Peterson, A. A. Departures from the Adsorption Energy Scaling Relations for Metal Carbide Catalysts. *J. Phys. Chem. C* **2014**, *118*, 13026–13034.
(30) Greeley, J.; Jaramillo, T. F.; Bonde, J.; Chorkendorff, I.; Nørskov, J. K. Computational High-Throughput Screening of Electrocatalytic Materials for Hydrogen Evolution. *Nat. Mater.* **2006**, *5*, 909–913.

TOC Graphic

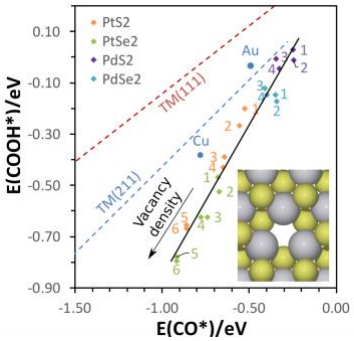
PtS2
PtSe2
PdS2
PdSe2
TM(111)
TM(211)
Au
Cu
Vacancy density
E(COOH*)/eV
E(CO*)/eV
0.10
-0.10
-0.30
-0.50
-0.70
-0.90
-1.50
-1.00
-0.50
0.00